RFID-Based Wireless Passive Sensors Utilizing Cork Materials

Ricardo Gonçalves, *Student Member, IEEE,* Sergi Rima, Roberto Magueta, Pedro Pinho, *Member, IEEE,* Ana Collado, *Senior Member, IEEE,* Apostolos Georgiadis, *Senior Member, IEEE,* Jimmy Hester, *Student Member, IEEE,* Nuno B. Carvalho, *Fellow, IEEE,* and M. M. Tentzeris, *Fellow, IEEE,*

***Abstract*—This paper presents the design of low cost, conformal UHF antennas and RFID tags on two types of cork substrates: natural cork and agglomerate cork. Such RFID tags find application in wine bottle and barrel identification and additionally they are suitable for numerous antenna-based sensing applications.**

This work includes the high frequency characterization of the selected cork substrates considering the anisotropic behavior of such materials. Plus, the variation of their permittivity value as a function of the humidity is also verified.

As a proof-of-concept demonstration, three conformal RFID tags have been implemented on cork and their performance has been evaluated using both a commercial Alien ALR8800 reader and an in-house measurement setup. The reading of all tags has been checked and a satisfactory performance has been verified, with reading ranges spanning from 0.3 m to 6 m. Also, this paper discusses how inkjet printing can be applied to cork surfaces and an RFID tag printed on cork is used as humidity sensor. Its performance is tested under different humidity conditions and a good range in excess of 3 m has been achieved, allied to a good sensitivity obtained with a shift of more than 5 dB in threshold power of the tag for different humid conditions.

***Index Terms*—UHF RFID, cork characterization, passive sensor, humidity sensor, wireless sensor, inkjet printing**

I. Introduction

RFID technology has been applied in an increasing number of applications ranging from identification and localization to various types of monitoring and sensing [1]. The large and diverse number of application scenarios has resulted in various challenges for the tag design, which include the use of a diverse range of substrate materials such as paper, plastic (PET) [1], plywood [2], to name a few, as well as the use of different fabrication techniques targeting large volume production such as inkjet printing [3], and consideration of low cost conductive materials such as paperclips [3].

A characteristic example of the requirement for low-profile, conformal RFID tags is related to liquid bottle tagging, including water, wine as well as a variety of other liquids. The challenge for conformal and low-profile antennas, has led to different designs, such as a meander monopole placed inside a hollow plastic bottle closure [4], and several designs consisting of dipole antennas placed around the bottle plastic or glass neck [5], [6] or body [7].

This paper is a more in-depth analysis and an extension of the work presented at [8], [9]. In this work we discuss in detail the design and analysis of the UHF tag antennas proposed in the symposium papers and how the presented solutions are viable for efficient bottle tagging. We also propose a possible implementation of a humidity sensor using the supporting cork as the sensing element.

RFID has been used as the foundation technology for the implementation of several passive remote sensors for different application scenarios, from temperature to chemical sensors [10]. The basic techniques to perform sensing in a wireless way are usually based on resonant frequency shifts [11] and/or wake-up power changes of the passive tags [12].

Temperature sensing using passive RFID tags has been explored in [11]–[13], in the first and second cases by using substrates with permittivity sensitive to the temperature changes, while in the third case thermistors are used in the tag matching network to shift the resonant frequency of the tag according to the temperature.

Instead of just temperature measurements, in [14] a combined temperature and humidity sensor is explored. In this case a proposal for HF and UHF sensor tags is presented. A micro-controller is used to interface a RFID chip and the sensor elements or ICs responsible for the temperature and humidity measurements. The micro-controller reads the data from the sensors and writes it in the RFID chip memory, which is then accessed with a regular RFID reader. This solution seems to be the most mature and most reliable although it is also the more expensive. It has been also considered for harsh environments but it is severely dependent on the packaging which may affect the accurate temperature and humidity sensing in many scenarios.

Other sensing capabilities are explored in [15] and [16]. In

This work was supported by the Portuguese FCT/MCTES by financing the PhD grant SFRH/BD/91249/2012 and the project CREATION EXCL/EEI-TEL/0067/2012. This work was performed under the framework of EU COST Action IC1301 Wireless Power Transmission for Sustainable Electronics (WIPE).

This work was also supported by the Spanish Ministry of Economy and Competitiveness and FEDER funds through the project TEC2012-39143, the EU Marie Curie FP7-PEOPLE-2009-IAPP 251557.

R. Gonçalves, N. B. Carvalho and R. Magueta are with the Instituto de Telecomunicações and the Department of Electronics, Telecommunications and Informatics, University of Aveiro, Campus Universitario de Santiago, 3819-193 Aveiro, Portugal (e-mails: rgoncalves@av.it.pt; nbcarvalho@ua.pt; rlm@ua.pt).

P. Pinho is with the Instituto de Telecomunicações, Campus Universitario de Santiago, 3819-193 Aveiro, Portugal and the Instituto Superior de Engenharia de Lisboa, 1959-007 Lisboa, Portugal (e-mail: ppinho@deetc.isel.pt).

S. Rima, A. Collado and A. Georgiadis are with the Department of Microwave Systems and Nanotechnology, Centre Tecnologic de Telecomunicacions de Catalunya (CTTC), 08860 Castelldefels, Spain (e-mail: srima@cttc.es; acollado@cttc.es; ageorgiadis@cttc.es).

J. Hester and M. M. Tentzeris are with the School of Electrical & Computer Engineering (ECE) and the Georgia Electronic Design Center (GEDC), Georgia Institute of Technology, Atlanta, GA, USA (e-mail: jimmy.hester@gatech.edu; etentze@ece.gatech.edu).

the first case a passive sensor for pH of solutions is presented. This one is based on HF RFID approach, by connecting pH sensing electrodes in parallel to an inductive coil which will result in a resonant frequency shift of the coil. Every measured resonant frequency value is matched to a specific pH level of the target solution. A temperature-dependent resistor is used in parallel with a varactor and the electrodes and coil in order to monitor the temperature. Temperature shifts will impose a change in the quality factor of the coil which can be detected therefore allowing a temperature compensated pH measurement. In [16] a microfluidic channel are used to create a varactor sensor for chemicals which are introduced into an UHF RFID tag antenna. These microfluidic structures impose a resonant frequency shift of the antenna for different chemicals, therefore allowing the detection of certain substances using passive remote sensing.

In addition to its application in wine and bottle industry, cork material has found increasing applicability as an insulator in various fields, including space technology, due to characteristic properties such as lightweight and low thermal conductivity [17]. Therefore the characterization of this material and the successful design of antennas and circuits in it might open the door for many diverse and interesting applications.

There are several ways to etch the cork with conductive materials in order to fabricate the antennas or circuits on cork. Standard milling fabrication is used to transfer the antenna design on a low cost adhesive copper tape, which is then attached to the cork substrate, allowing for a fast and cost effective fabrication. Another possible implementation is the use of inkjet printing, if care is taken to create a coating on the cork that has enough surface energy to sustain the ink in place.

This paper describes the dielectric properties of cork and introduces the cork as a possible substrate for the implementation of antennas at high frequencies and explores its use for sensing of humidity. This document is organized as follows. In the following section the electrical properties of two types of cork samples are characterized. The permittivity and loss factor of a natural cork sample and a fabricated pressed agglomerated cork sample are extracted with two characterization methods for comparison purposes. Section III shows the design of three different antennas for passive RFID tags to be embedded into barrels or bottles for inventory. Section IV presents the measurement setup and the measured results for all the proposed tags. Section V investigates the permittivity shift with humidity variation and shows a possible implementation of a passive humidity sensor based on RFID using cork as the sensitive mechanism. Finally, section VI draws the main conclusions about this work.

II. Cork permittivity and loss estimation

Antenna design requires knowledge of the electrical properties of the materials which comprise the antenna topology; in the case of cork, its electrical properties have been relative unknown in the RF frequency range.. Moreover, through visual inspection of the cork material and given the structure of the material of the cork laminates, we expect to see an an anisotropic behavior of the dielectric material. Therefore, different orientations should be considered when analyzing cork's electrical properties.

A. Permittivity and loss estimation: Theory

In order to estimate the permittivity and loss tangent of the cork we used transmission/reflection methods based on microstrip transmission lines.

The method utilized to characterize the cork is based on the measurement of S parameters of two different length lines, as described in [18], [19]. For the implementation of the given method two microstrip lines with the same characteristic impedance (not necessarily 50 Ω), that is, same width and slightly different lengths are fabricated with the Material Under Test (MUT) as substrate. The permittivity is estimated based on the measurement of the propagation constant, γ, of both lines and relating the unwrapped propagation phase constant, β, with the propagation phase constant in vaccum, k_0.

$$\varepsilon_{r,eff} = \left(\frac{\beta}{k_0}\right)^2 \tag{1}$$

The loss tangent in this case is calculated according to (2) as described in [20] and assuming the entire transmission line losses are due to the dielectric, which is not entirely true but provides a reasonable estimation of the loss tangent value.

$$\tan\delta = 0.0366\frac{\alpha\lambda_0\sqrt{\varepsilon_{r,eff}}(\varepsilon_r - 1)}{\varepsilon_r(\varepsilon_{r,eff} - 1)} \tag{2}$$

where α is the losses obtained from the propagation constant measured, λ_0 is the wavelength, $\varepsilon_{r,eff}$ is the effective dielectric constant of the substrate and ε_r is the relative permittivity of the material.

B. Permittivity and loss estimation: Measurements

There are numerous types of cork materials that are used for the elaboration of wine cork bottle stoppers (Fig. 1). Among them we can disguise the wine corks punched directly from a panel of natural cork and the ones fabricated with pressed or agglomerate cork. Apart from the fabrication method, these types of corks can be distinguished easily by visual inspection, as can be seen in Fig. 1 and 2. In this section we demonstrate the permittivity and loss factor calculation for the above cork type materials.

The microstrip lines utilized for material characterization are shown in Fig. 2, where the difference in their respective lengths is quite clear, in a similar way as proposed in [18], [19], [21]. Due to the expected anisotropic behavior of the cork, which is confirmed by the results shown in Fig. 3, slices of the material were cut in two different directions: axial and radial.

S-parameter measurements were performed on both pairs of microstrip lines of lengths l_1 and l_2, being l_1 of 15 mm and l_2 of 25 mm. One pair of microstrip lines were placed on the cork substrate corresponding on the axial axis cut and the other to the radial one. The conducting strips were fabricated by milling of adhesive copper tape, with 35 μm thickness and

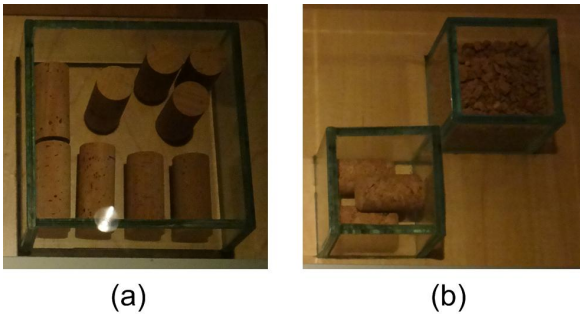

Fig. 1. Two different types of wine bottle corks (a) natural cork (b) agglomerated cork.

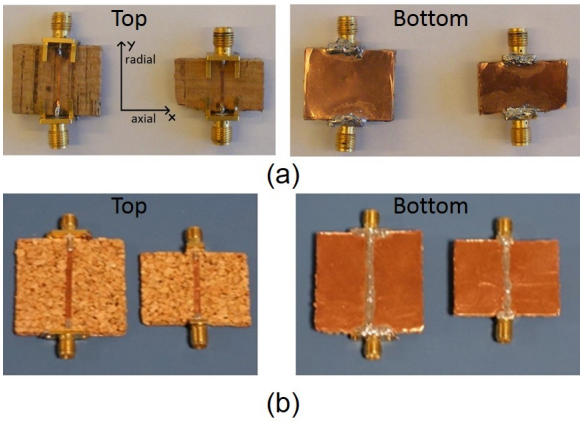

Fig. 2. Photograph of two microstrip lines placed on (a) natural and (b) agglomerate cork substrate.

4.7×10^8 S/m conductivity, and placing them on the cork samples. SMA connectors were soldered to the edges of the microstrip lines for interfacing.

A vector network analyzer from Agilent Technologies with reference E8361A was used to perform the two-port S-parameters measurements in the frequency range from 750 to 950 MHz. The estimated permittivity for the cork is depicted in Fig. 3.

The measured permittivity for the cork is rather low, with values ranging between 1.49 and 1.91, which was expected due to the existing air gaps in the cork [17]. Another characteristic that can be easily observed in the depicted results is the anisotropic (permittivity is different for different directions) behavior of the natural cork in contrast with the nearly isotropic (permittivity is the same in both axis) behavior of the agglomerate cork. This is mainly due to the random distribution of the cork pieces on the agglomerate cork, in comparison to the clearly stratified structure of the natural cork. The lower permittivity of the agglomerate cork is also explained by the larger number of air gaps in its slabs, which is clear from the photographs in Fig. 2.

The isotropy/anisotropy of the the different cork materials is also clear in the loss tangent values. The measured losses for the natural cork are different over different directions while they are roughly the same for the agglomerate cork. Besides, the dissipation factor of the agglomerate cork is slightly lower than the natural cork, as shown in Fig. 3. This indicates

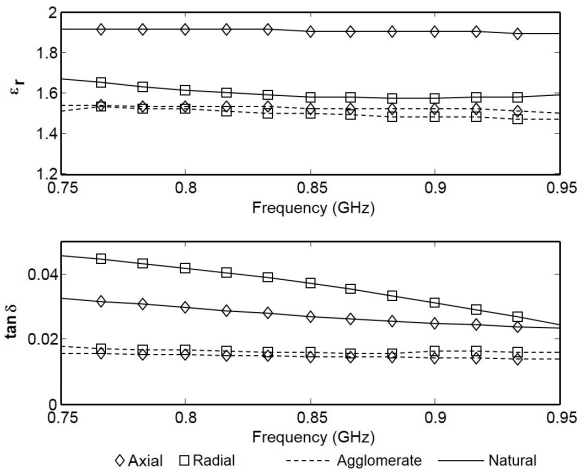

Fig. 3. Measured dielectric constant and loss tangent of axial and radial samples of natural and agglomerate cork in the range from 750 to 950 MHz.

that agglomerate cork might be a better candidate for use in antennas and microwave circuits applications.

After the characterization of the cork materials up to 950 MHz, we were able to incorporate them on CST and use them to simulate various UHF RFID tag antennas as described in the following sections.

III. UHF RFID TAG ANTENNAS

In this section, three different types of UHF RFID tag antennas are presented. The first one is a meandered dipole antenna wrapped around a cork cube to be placed inside a barrel cork stopper. The second design is a compact design based on a meandered monopole antenna to be placed inside a bottle cork stopper. The third prototype is a miniaturized configuration of a dipole antenna, achieved by reducing the antenna to the matching ring and a lumped component. This is wrapped around the surface of a regular bottle cork stopper. In the last two approaches the glass bottle filled with water were included in the simulation model in order to better match the real operation environment where the antenna will be placed.

A. RFID tag for barrel cork stopper

As a proof of concept and without loss of generality, a compact meandered dipole antenna was designed and modeled to fit in a barrel cork. The designed prototype, that is shown in Fig. 4, uses a cubic shape in order to facilitate the cutting of the material. It was made with natural cork, the most commonly used for barrel cork stoppers.

When meandering the dipole arms, the direction of the current flow in the radial direction of the dipole is inverted, so to some extent these currents cancel when viewed from far field and effectively do not contribute to radiation [22]. Additionally, a meandered structure features a significantly smaller inductance per unit length than a straight dipole and since the resonant frequency of the antenna is inversely proportional to the product of inductance and capacitance when these are reduced, the resonant frequency is increased,

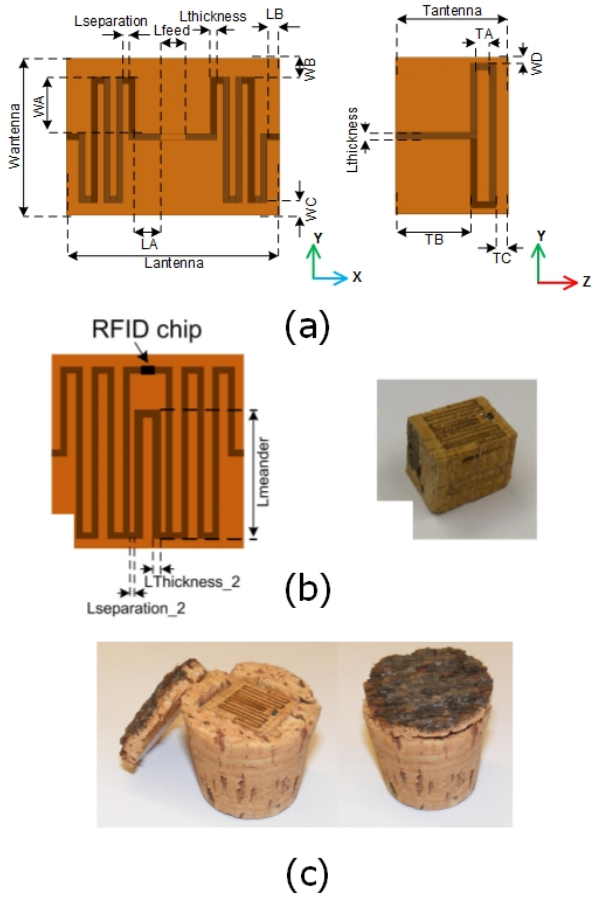

Fig. 4. Compact meandered dipole antenna (a) Dimensions of the compact meandered dipole antenna matched to 50 Ω, (b) with matching inductive ring matched to the RFIC, (c) photograph of the implemented prototype.

TABLE I
MEANDERED DIPOLE ANTENNA DIMENSIONS

Parameters	sizes (mm)
$L_{thickness}$, L_{feed}	0.75, 4.0
$L_{separation}$, $W_{antenna}$	1.0, 25.0
$L_{antenna}$, $T_{antenna}$	32.0, 18.0
L_A, L_B, W_A	4.0, 2.0, 9.0
W_B, W_C, W_D	3.0, 2.0, 1.0
T_A, T_B, T_C	2.0, 12.0, 2.0
$L_{separation\_2}$, $L_{thickness\_2}$	0.65, 1.15
$L_{meander}$	14.0

which means that for the same total length, a meandered dipole has a higher resonant frequency than a straight dipole. This change in the resonant frequency was considered and the design of the compact meandered antenna, the dimensions of which are reported in Table I, were modified to re-tune the resonant frequency.

The compact cubic antenna shown in Fig. 4 (a) was initially designed to be matched to 50 Ω. An RFIC chip was then connected to the compact meandered dipole antenna, and a loop ring is inserted around the chip making the connection to the dipole arms, as shown in Fig. 4 (b). The selected chip is the Higgs 3 from Alien Technology. This IC is EPCglobal Gen2 and ISO/IEC 1800-6c compliant, requires low power to perform the reading operation and operates in the RFID UHF

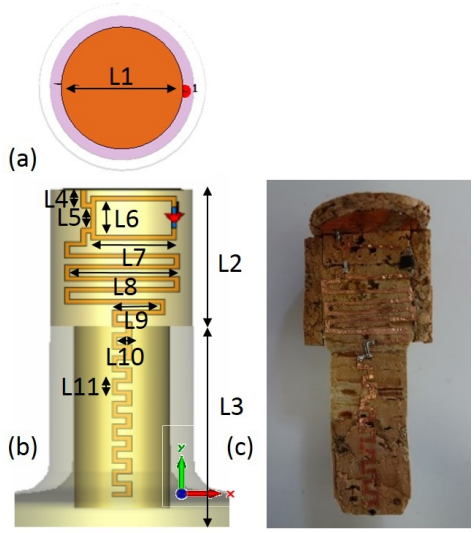

Fig. 5. Agglomerate Cork RFID antenna (a) top view (b) front view and (c) photograph.

TABLE II
MEANDERED MONOPOLE ANTENNA DIMENSIONS

Parameters	sizes (mm)
L_1, L_2, L_3	26.0, 30.0, 40.0
L_4, L_5, L_6	3.0, 4.5, 7.4
L_7, L_8, L_9	17.0, 23.0, 10.0
L_{10}, L_{11}	3.0, 3.5

bands (860-960 MHz). The input impedance of the RFID chip can be modeled as a series equivalent circuit with a resistance R of 1500 Ω in parallel with a 0.9 pF capacitor C, which results in a complex input impedance at 866 MHz of 27.35 - j200.5 Ω.

B. RFID tag for bottle cork stopper

In this subsection we used agglomerate pressed cork and designed an antenna for an RFID tag that could be inserted into a cork stopper for a wine bottle.

It was necessary to reduce the size of the antenna when compared to the previous topology in order to make it fit into a typical wine bottle. Therefore, we opted to make a monopole instead of a dipole. The proposed RFID tag antenna design for the wine bottle cork stopper is depicted in Fig. 5.

As we can see from the picture the antenna is connected to a conductive circular disk on the top of the cork stopper that functions as a ground plane. Similar to the previous case, there is an inductive loop at the feed point, in order to match the antenna to the complex input impedance of the chip. In this case, a UCODE SL3ICS1002 from NXP was used, which has an input impedance of 16-j158 Ω at 866 MHz.

The dimensions of this antenna are presented in Table II.

The radiation pattern is essentially omnidirectional which was expected considering the antenna geometry. This can be observed in the simulation results depicted in Fig. 6 (a). However, this is true when the bottle is empty. The simulation model was designed with a glass (ε_r=4.8) bottle with a thickness of 6 mm, which is the thickness of the glass measured

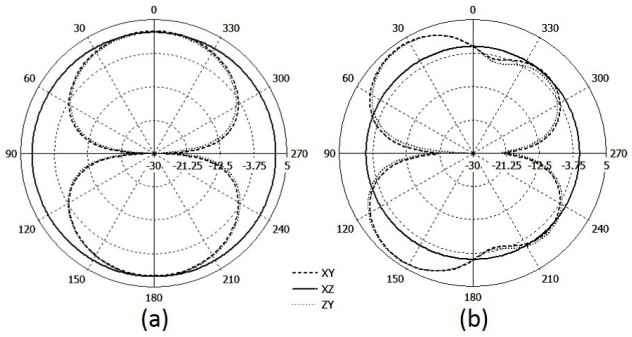

Fig. 6. Simulated radiation patterns of the meandered monopole RFID antenna (a) with empty bottle (b) with filled bottle

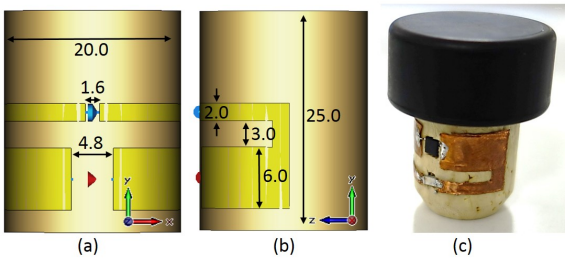

Fig. 7. Agglomerate Cork RFID antenna (a) front view (b) left-side view, (c) prototype photograph. All dimensions in mm.

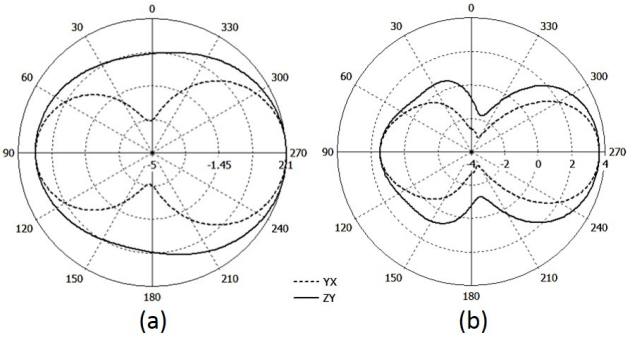

Fig. 8. Simulated radiation pattern of the conformal RFID tag considering (a) only the bottle neck (b) full filled bottle.

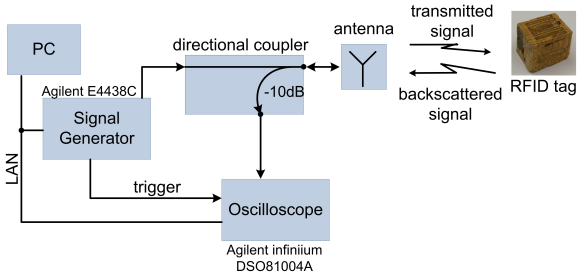

Fig. 9. RFID read range measurement setup.

from a typical wine bottle. The presence of liquid inside the bottle has a considerable effect on the radiation pattern, which is shown in Fig. 6 (b). For simulation purposes, water was considered inside the bottle. Most beverages are mainly composed of water, which means that for electromagnetic simulation purposes it will render similar results as wine. Water has an estimated permittivity of 78.3 at 25 °C [23]. The water is set at a distance of around 15 mm of the stopper edge.

Nevertheless the gain of the antenna remains essentially the same in both cases. The monopole antenna was optimized to work in the filled bottle, therefore, when the bottle is empty there is a slight mismatch in the antenna impedance. This allied to the smaller directivity of the radiation on the empty bottle, result in a total efficiency that is very close to the one achieved in the filled bottle case, even with the lower radiation efficiency occurring from the liquids absorption.

This prototype has rather large dimensions that extrude the top of the bottle. Due to the visual impact we decided to reduce the size of the antenna further in order to make it fit into regular bottle stoppers. The proposed prototype was designed in order to fit on the surface of a regular T-cork stopper, which is a stopper commonly found on liquors, that provides a secure grip while applying little deformation to the antenna.

The proposed prototype is presented in Fig. 7.

In order to miniaturize the antenna an SMD resistor of 6.2 Ω is used in the impedance matching ring in order to reduce the size while maintaining a good matching of the antenna impedance. This of course dissipates a great deal of the input power, therefore reducing the overall efficiency of the antenna in 90%. However, the impedance mismatch before the insertion of the resistor corresponds to a reflection of $\Gamma = 0.98$, which results in a total efficiency below 1%, that is effectively lower when compared to the efficiency with the resistive element, which is around 5%.

The antenna is simulated in two different scenarios, an empty and a water filled bottle, for comparison. The bottle is designed considering a thickness of 8 mm of glass, which is a typical value for wine bottles, where the glass is modeled with the default values from the simulator library, with a permittivity of 4.82. The presence of the liquid has a large influence in the radiation pattern and also in the total efficiency, due to the fact that water absorbs electromagnetic energy [24]. The changes of the radiation pattern of the antenna when considering the empty bottle versus the liquid filled bottle is depicted in Fig. 8.

Due to the radiation efficiency reduction in this prototype the reading range of the tag is considerably reduced.

IV. RFID TAGS MEASUREMENTS

The read range of the designed RFID tags was tested using a signal generator, an oscilloscope or a vector signal analyzer (VSA) and an antenna that is used for transmit and receive using a directional coupler, as depicted in Fig. 9. In order to evaluate the distance of communication with the tag, a query is sent to the tag and the back-scattered response is analyzed to see if a modulation is discernible.

The back-scattered signal from the RFID tag is received by the digital oscilloscope which can be configured to perform the FFT over the received time window and show the frequency spectrum. A VSA can also be used to check the frequency spectrum. Since the tag uses amplitude shift keying (ASK)

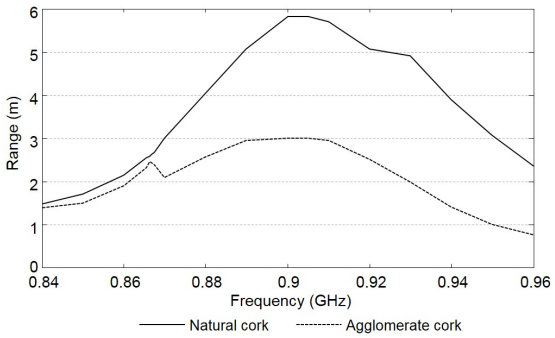

Fig. 10. Read range for the natural cork and agglomerate cork RFID antenna.

to modulate the back-scatter signal, the presence of the tag response is discerned by the presence of sub-carriers around the interrogation carrier.

In order to determine the read range, a fixed distance between the antenna and the RFID tag is set (d=38 cm) and then the transmitted power from the generator is varied to find the minimum threshold power (P_{th}) necessary to turn on the tag. The read range for a given transmitted power ($EIRP$) can be determined using the following expression [25]

$$r = d\sqrt{\frac{EIRP}{P_{th}LG_t}} \tag{3}$$

where L are the losses in the cables and G_t is the gain of the transmitting antenna (since only one antenna is being used).

The maximum read range for different operation frequencies and for a EIRP maximum of 1 W was determined using this method. Fig. 10 shows ~~that~~ the maximum reading ranges obtained for the barrel cork stopper tag and the bottle cork stopper tag. For both cases, the peak reading range occurs around 900 MHz, corresponding to nearly 6 m for the barrel stopper and 3 m for the bottle cork stopper.

The range of the bottle stopper tag is smaller than that of the barrel stopper tag. However, we need to consider that the bottle cork stopper was tested in a real application scenario, inserted into a water (which is similar to wine in terms of electromagnetic properties and effects on radiation) filled bottle, while the barrel stopper was tested by itself, outside any barrels and without any liquids in its vicinity.

The third prototype, the miniaturized bottle stopper tag, showcased the smallest reading range. This is mainly due to the smaller efficiency of the antenna. The reading range of the considered prototype in an application scenario condition, that is, inserted into a water filled glass bottle, was of 0.3 m at 866.6 MHz, achieved for the maximum output power (30 dBm) of a commercial RFID reader. However, this reading range is obtained regardless of the orientation of the bottle. That is, either if the bottle is placed horizontally or vertically, the reading range obtained in the maximum direction of radiation is the same.

Although small, the reading range obtained is rather acceptable if we consider the following application scenarios. In the first case during bottling process, the RFID reader antennas can be mounted in a platform hanging over the

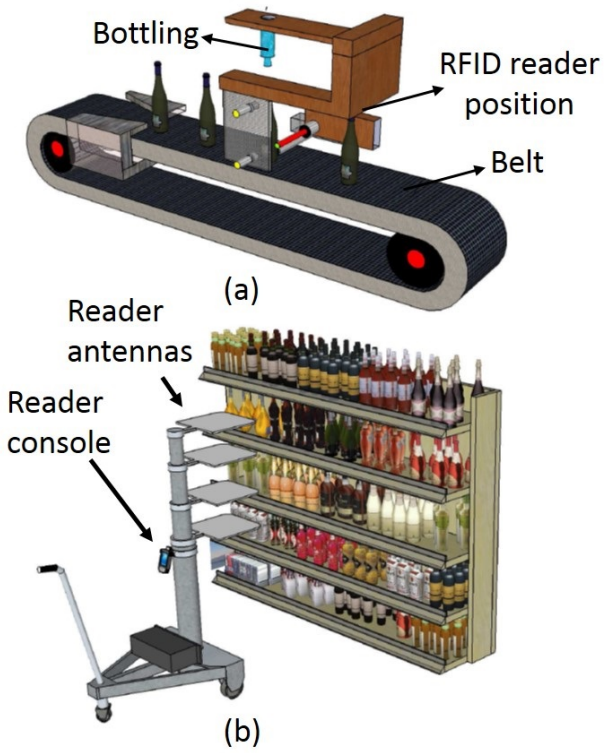

Fig. 11. Scenarios of application of the bottle stopper tag and reading solutions (a) at bottling stage, (b) at distribution stage in supermarket.

belt that circulates the bottles around the bottling facilities, as illustrated in Fig. 11 (a). On a distribution scenario, for instance, on supermarket shelves, the readings can be obtained by an emplyee with a portable reader, which points the reader to the shelves, as illustrated in Fig. 11 (b). In both cases the readings are obtained in close vicinity to the bottles, therefore we can say that the reading ranges obtained with the considered tags, although small, are acceptable.

It is important to note that the work presented in this paper is meant as a proof of concept. That is, this investigation goes into the development of possible RFID tag antennas that can work within the vicinity of liquids while inserted into glass bottles. When we consider the possibility of industrialization of these designs, some issues arise, which can only be tackled with a careful design having into consideration the cork manufacturing and the bottling processes. For instance, the bottle tag of Fig. 5 is not a common shape cork stopper, therefore, a new cork stopper model would need to be used and the bottling processes would need to adapt to this new shape, besides, the manufacturing process of the cork stopper would also need to be changed. In the case of the tag in Fig. 7, due to it's application on the surface of the cork and it's compact size, it can be used with common shaped stoppers. However, since it is located on the surface, it requires some cover material around the cork, which is not advisable. Besides, it requires the bottling to be done slowly and with little pressure, contrary to what is the current bottling process.

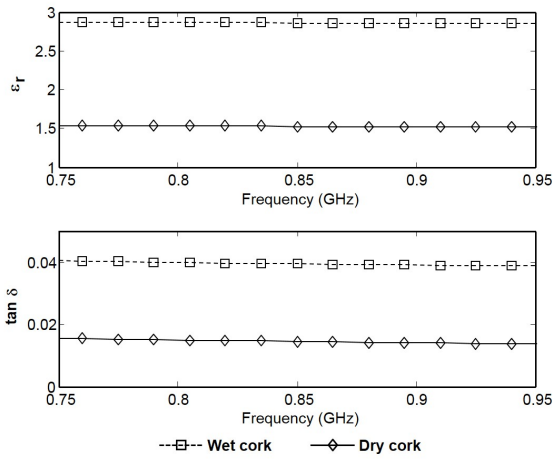

Fig. 12. Measured permittivity of the dry and wet cork applying the two-line method with two different length microstrip lines.

V. Humidity Sensors Based on Cork

In order to develop a passive humidity sensor, we're using cork as the sensing surface. Cork is a porous dielectric material, and as such, it absorbs water. This results in a material that is sensitive to humidity changes. In order to determine to which extent the cork permittivity changes with the difference in water content, permittivity measurements were performed on the dry and soaked cork slabs, using the two-line method, according to [19], with microstrip lines. The effective permittivity values are presented in Fig. 12.

We can see that the permittivity changes considerably, between 1.5 when dry to 3 when in wet condition, which proves the water absorption properties of the cork. Besides, we can also observe an increase in the losses, from around 0.015 when dry to 0.04 when wet.

In order to develop the passive sensor we designed an UHF RFID antenna inserted in between two cork slabs. The antenna was developed with inkjet printing, using conductive silver based ink by ANP.

In order to be able to print the ink on top of the cork, a coating surface has to be created so that it doesn't absorb the ink. Epoxy and SU-8 were used for this purpose. By placing a slim layer of epoxy on the surface of the cork we were able to create a smoth surface for printing. Then SU-8 was printed on top of the epoxy in order to create a surface with high enough tension to sustain the ink in place.

The simulated prototype comprised three different dielectric layers. An epoxy layer on top of which the antenna was printed and then two different layers which emulate the cork. A slim fixed permittivity cork slice which accounts for the fact that not all the dielectric cork slab will absorb water and an outside slab with varying permittivity which is going to change based on the humidity. The proposed prototype is shown in Fig. 13. The antenna was designed to match the input impedance of a Higgs 4 RFID chip from Alien at 915 Mhz, which corresponds to 18.4+j181.2 Ω. The size and placement of the inductive ring is determined according to the guidelines from [26].

In order to access the behavior of the tag, the minimum

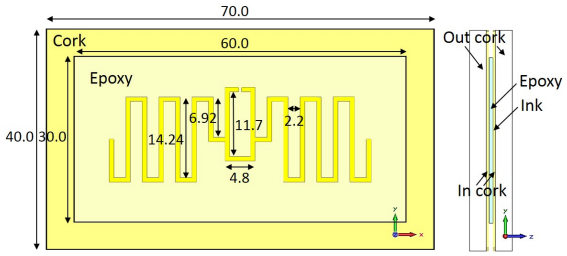

Fig. 13. Proposed RFID tag using cork slabs prototype. All dimensions in mm.

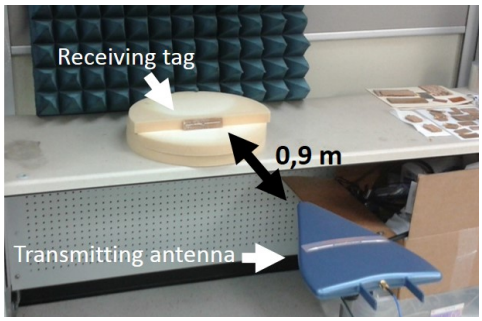

Fig. 14. Measurement setup.

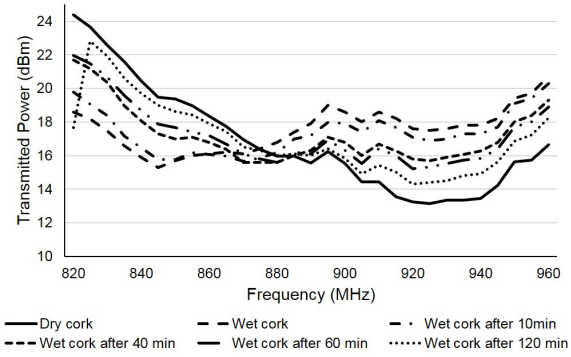

Fig. 15. Minimum transmitted power to activate the prototype tag with different wetting conditions.

threshold power to turn on the tag is measured at each frequency. For that purpose a more easy setup was used, with the Voyantic Tagformance 7, RFID test equipment. A picture of the measurement scenario is shown in Fig. 14. The frequency at which the tag presents the lowest turn on power corresponds to the frequency at which the antenna has the better match to the chip input impedance. The measured threshold power of the tag is shown in Fig. 15.

By looking to the transmitted power measurements it is easy to identify a shift in the matched resonance of the antenna to the chip for different humidity values. It is also possible to just look into the turn on power at a single frequency and match the minimum power level required to a given humidity level. Considering the relative humidity levels inside the lab were of 60%, we can see that there is a large and easily traceable power shift up to ≈100% at 920 MHz, which is the frequency at which the antenna is matched for the dry cork condition.

Still on the plot from Fig 15 we can see that when the cork

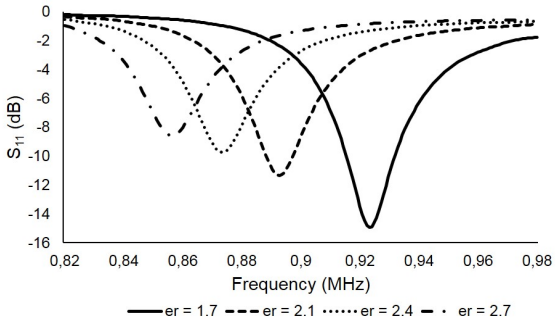

Fig. 16. Simulated reflection coefficient of the sensor tag antenna for different permittivity values of the outside cork slabs.

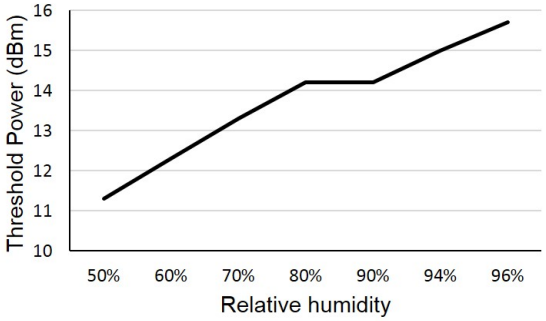

Fig. 17. Threshold power variation with humidity measured within the thermal chamber with humidity control.

becomes wet, the best matched frequency is around 845 MHz, which matches with the simulation prediction for the wet condition. The simulated reflection coefficient, of the sensor tag antenna for different permittivity values of the outside slabs, is depicted in Fig. 16.

Comparing the simulation and the measurements we can see a relationship between the threshold power to turn on the tag and the reflection coefficient of the sensor tag antenna. For a permittivity of 1.7, which corresponds to the near dry cork, the resonant frequency is around 920 MHz where a good match (reflection coefficient at -15 dB) is obtained, which correlates to the lowest threshold power measured, happening for the dry cork at 920 Mhz. While for a permittivity of 2.8, which is almost the value obtained for ≈100%, the resonance is around 850 MHz with a poor match (reflection coefficient at -8 dB), which correlates to the wet condition with the lowest threshold happening at 845 MHz with 3 dB difference to the dry condition.

Another measurement was performed inside a thermal chamber with humidity control. The threshold power was measured at 915 MHz for different humidity conditions. There's a threshold power difference of roughly 4.4 dB, between 50 to 96% relative humidity. The threshold power variation with humidity is shown in Fig. 17.

This behavior confirms the response obtained for the previous measurements by spraying and drying the cork. The threshold power difference, between this measurement and the one shown in Fig. 15, is due to the propagation environment in which the measurements were made. The thermal chamber has metallic walls, therefore the propagation inside is unknown and random with multiple reflections happening. For that reason the frequency sweep was not performed and an accurate threshold power can't be obtained, since the propagation environment is very different from open space.

VI. Conclusion

In this paper, three types of RFID tags implemented in cork based substrates have been presented. These RFID tags aim to be used in wine bottles or barrels integrated in their cork stoppers for inventory and monitoring of bottled beverages. One of the contributions of this paper is the dielectric characterization of natural and agglomerate pressed cork. It is shown that this material has a very low dielectric constant and also a reasonable dissipation factor that makes it suitable to the design and implementation of printed antennas for different applications. The RFID tags proposed in this paper have shown a very good result in terms of reading ranges while maintaining conformity with the targeted application dimensions constraints. The proposed RFID tag for bottle labeling is small enough to fit regular cork bottle stoppers and shows a reading distance of 30 cm, which for the application envisioned is an acceptable value.

Cork is also explored as a possible way to implement an humidity sensor. Its properties are explored and it is shown that cork has a considerable sensitivity to the water contents due to its absorption characteristic. A passive humidity sensor can be developed taking advantage of these properties and using RFID technology.

References

[1] A. Rida., L. Yang, and M. Tentzeris, *RFID-Enabled Sensor Design and Applications*. Artech House, 2010.

[2] J. Virkki, J. Virtanen, L. Sydanheimo., L. Ukkonen, and M. M. Tentzeris, "Embedding inkjet-printed antennas into plywood structures for identification and sensing," *Proc. 2012 IEEE International Conference on RFID Technologies and Applications*, pp. 34–39, November 2012, 2012.

[3] P. V. Nikitin, S. F. Lam, and K. V. S. Rao, "Rfid paperclip tags," *Proc. IEEE Int. Conf. on RFID*, pp. 162–169, April 2011, 2011.

[4] Z. Hu and P. H. Cole, "Bottle packaged wine product detection by uhf rfid systems," *Proc. Int. Conf. on Electromagnetics in Advanced Applications*, pp. 301–304, September 2010, 2010.

[5] Y. D. Kim, "Design of near omnidirectional uhf rfid tag with one-off seal function for liquid bottles," *Wiley Microwave and Optical Technology Letters*, vol. 55, pp. 375 – 379, 2013.

[6] J. Xi and T. T. Ye, "Conformal uhf rfid tag antenna mountable on winebottle neck," in *Proc. IEEE Antennas and Propagation Soc. Int. Symp.*, July 2012.

[7] T. Bjorninen, A. Z. Elsherbeni, and L. Ukkonen, "Low profile conformal uhf rfid tag antenna for integration with water bottles," *IEEE Antennas Wireless Propag. Lett.*, vol. 10, pp. 1147 – 1150, 2011.

[8] R. Goncalves, S. Rima, R. Magueta, A. Collado, P. Pinho, N. B. Carvalho, and A. Georgiadis, "Rfid tags on cork stoppers for bottle identification," *IEEE International Microwave Symposium*, Tampa, FL, 1-6 June, 2014.

[9] R. Goncalves, R. Magueta, P. Pinho, and N. Carvalho, "Rfid passive tag antenna for cork bottle stopper," in *Antennas and Propagation Society International Symposium (APSURSI), 2014 IEEE*, July 2014, pp. 1518–1519.

[10] S. Kim, C. Mariotti, F. Alimenti, P. Mezzanotte, A. Georgiadis, A. Collado, L. Roselli, and M. M. Tentzeris, "No battery required: Perpetual rfid-enabled wireless sensors for cognitive intelligence applications," *IEEE Microw. Mag.*, vol. 14, pp. 66 – 77, 2013.

[11] H. Cheng, S. Ebadi, and X. Gong, "A low-profile wireless passive temperature sensor using resonator/antenna integration up to 1000 °c," *IEEE Antennas Wireless Propag. Lett.*, vol. 11, pp. 369 – 372, 2012.

[12] J. Virtanen, L. Ukkonen, T. Bjorninen, L. Sydanheimo, and A. Z. Elsherbeni, "Temperature sensor tag for passive uhf rfid systems," *Sensors Applications Symposium (SAS), IEEE*, pp. 312 – 317, February 2011.

[13] D. Girbau, A. Ramos, A. Lazaro, S. Rima, and R. Villarino, "Passive wireless temperature sensor based on time-coded uwb chipless rfid tags," *IEEE Trans. Microw. Theory Tech.*, vol. 60, pp. 3623 – 3632, 2012.

[14] P. Pursula, I. Marttila, K. Nummila, and H. Seppa, "High frequency and ultrahigh frequency radio frequency identification passive sensor transponders for humidity and temperature measurement within building structures," *IEEE Trans. Instrum. Meas.*, vol. 62, pp. 2559 – 2566, 2013.

[15] S. Bhadra, D. S. Y. Tan, D. J. Thomson, M. S. Freund, and G. E. Bridges, "A wireless passive sensor for temperature compensated remote ph monitoring," *IEEE Sensors J.*, vol. 13, pp. 2428 – 2436, 2013.

[16] B. S. Cook, J. R. Cooper, and M. M. Tentzeris, "An inkjet-printed microfluidic rfid-enabled platform for wireless lab-on-chip applications," *IEEE Trans. Microw. Theory Tech.*, vol. 61, pp. 4714 – 4723, 2013.

[17] S. P. Silva, M. A. Sabino, E. M. Fernandes, V. M. Correlo, L. F. Boesel, and R. L. Reis, "Cork: properties, capabilities and applications," *International Materials Reviews, Maney Publishing*, vol. 50, pp. 345 – 365, 2005.

[18] M. que Lee and S. Nam, "An accurate broadband measurement of substrate dielectric constant," *IEEE Microw. Guided Wave Lett.*, vol. 6, pp. 168–170, 1996.

[19] M. D. Janezic and J. A. Jargon, "Complex permittivity determination from propagation constant measurements," *IEEE Microw. Guided Wave Lett.*, vol. 9, pp. 76 – 78, 1999.

[20] D. M. Pozar, *Microwave Engineering*. John Wiley & Sons, 2012.

[21] F. Declercq, H. Rogier, and C. Hertleer, "Permittivity and loss tangent characterization for garment antennas based on a new matrix paencil two line method," *IEEE Trans. Antennas Propag.*, vol. 56, pp. 2548 – 2554, 2008.

[22] D. M. Dobkin, *The RF in RFID*. Newnes, 2nd Ed., 2012.

[23] C. G. Malmberg and A. A. Maryott, "Dielectric constant of water from 0○ to 100○c," *Journal of Research of the National Bureau of Standards*, vol. 56, pp. –, 1956.

[24] B. Wozniak and J. Dera, "Light absorption by water molecules and inorganic substances dissolved in sea water," in *Light Absorption in Sea Water*. Springer New York, 2007, vol. 33, pp. 11–81.

[25] K. V. S. Rao, P. V. Nikitin, and S. F. Lam, "Antenna design for uhf rfid tags: a review and a pratical application," *IEEE Trans. Antennas Propag.*, vol. 53, pp. 3870 – 3876, 2005.

[26] G. Zamora, S. Zuffanelli, F. Paredes, F. Martín, and J. Bonache, "Design and synthesis methodology for uhf-rfid tags based on the t-match network," *IEEE Trans. Microw. Theory Tech.*, vol. 61, pp. 4090 – 4098, 2013.